Original Article
Estimation and classification of temporal trends to support integrated ecosystem assessment

Hiroko Kato Solvang [ID] [1]* and Benjamin Planque [ID] [2]

[1]*Institute of Marine Research, Bergen, Norway*
[2]*Institute of Marine Research, Tromsø, Norway*

Corresponding author: tel: +47 48 22 04 78; e-mail: hirokos@hi.no.

We propose a trend estimation and classification (TREC) approach to estimating dominant common trends among multivariate time series observations. Our methods are based on two statistical procedures that includes trend modelling and discriminant analysis for classifying similar trend (common trend) classes. We use simulations to evaluate the proposed approach and compare it with a relevant dynamic factor analysis in the time domain, which was recently proposed to estimate common trends in fisheries time series. We apply the TREC approach to the multivariate short time series datasets investigated by the ICES integrated assessment working groups for the Norwegian Sea and the Barents Sea. The proposed approach is robust for application to short time series, and it directly identifies and classifies the dominant trends underlying observations. Based on the classified trend classes, we suggest that communication among stakeholders like marine managers, industry representatives, non-governmental organizations, and governmental agencies can be enhanced by finding the common tendency between a biological community in a marine ecosystem and the environmental factors, as well as by the icons produced by generalizing common trend patterns.

Keywords: common trend, Kalman filter, marine ecosystem, non-stationary time series modelling, polynomial regression model, stakeholders, state space model

Introduction

The integrated ecosystem assessment (IEA) is one approach to organizing scientific information at multiple scales and across sectors to support ecosystem-based fisheries management (EBFM) (Levin *et al.*, 2009). IEA aims to analyse and synthesize information on a wide range of ecosystem components and pressures and to identify status, changes, relationships, and processes at the ecosystem level (WKINTRA report, ICES 2018). The outcome of an IEA can take multiple forms, which generally include descriptions of the main interacting ecosystem, human components, and past changes in these components. Eventually, it also gives an assessment of the risks associated with possible future trajectories of the ecosystem.

This information can then be fed back into the design of dedicated observational efforts (monitoring plans), the definition of multi-sectorial management objectives, or the establishment of new indicators and associated reference points (Levin *et al.*, 2009, 2014; DePiper *et al.*, 2017).

There is a long history of making quantitative assessments of individual fish stocks, and with it, common vocabularies and practices that support efficient communication between natural scientists, managers, the fishing industry, and other interested stakeholders (Hilborn and Walters, 1992; ICES, 2013). Even when the numerical methods used to reconstruct individual fish stock histories are complex, the outputs of fish stock assessments are communicated in a standardized manner that can generally

be understood and used by different stakeholders. The same situation does not apply to IEAs, for which no methodological standards yet exist. Instead, many IEAs are still predominantly in the developmental phase, and a variety of methods have been explored. IEA results can reflect various aspects of an ecosystem beyond dynamics, status, and future risks, and they tend to be reported in an *ad hoc* fashion. For example, WKINTRA ICES (2018) reports using integrated trend analyses (ITA), which are used for IEA as a way to summarize changes that have occurred in recent decades in ecosystems in the north Atlantic and to highlight the possible connections among the physical, biological, and human ecosystem components. These methods cover graphical analyses as well as univariate and multivariate statistical analyses. Some methods have focused on individual components, while others have provided simplified representations of major past trends in the system or conveyed additional information on possible connections and causalities in the system. Unlike stock assessment models for which there are established benchmarking practices, no such practice exists for IEA. This can lead to ambiguous results or spurious interpretations, as was shown in the case of multivariate analysis applied to time series inappropriately (Kawasaki, 2004; Vanhatalo and Kulahci, 2016; Planque and Arneberg, 2018; Hallin *et al.*, 2018) or in the case of a statistical method applied to a short time series dataset (Hardison *et al.*, 2019; Solvang and Subbey, 2019). Therefore, to describe past changes in individual ecosystem components, more robust and theoretically correct trend analysis is required in IEA, and then the approach should be validated by benchmarking practices towards becoming a methodological standard.

Temporal changes in ecosystems can take the form of long-run movements—sometimes referred to as long-term trends or drifts—as well as short-/middle-run cyclic terms and noise components. The long-run changes entail a drift in time, a characteristic of temporal processes with a non-stationary mean (Kitagawa and Gersch, 1996). On the other hand, the cyclic and noise terms are considered stationary processes in the practical sense of time series analysis. When constructing statistical time series models, it is often useful to identify non-stationary trends and cyclic terms separately. Several structural time series models of this kind have been proposed in psychology and economics since the mid-1980s (Harvey, 1989; Kitagawa and Gersch, 1996; West and Harrison, 1997). When building multivariate time series models, it is also possible to decompose a non-stationary mean and cyclic components or seasonal components using a time series model (Kato *et al.*, 1994, 1996). Multivariate time series analysis has recently been used to model marine ecosystem dynamics (Solvang *et al.*, 2017) and to investigate population's dynamics through causal inference (Solvang and Subby, 2018; Solvang and Subbey, 2019).

In this article, we focus on modelling the *non-stationary mean trend* (hereafter called "trend"), which represents the long-run movements in observations. In particular, we focus on finding similar trends, called *Common trends*, which refer to similar long-term tendencies across ecosystem components. Identifying common trends can be useful as a diagnostic tool to reveal past changes and to explore the relationships among biological communities and between these communities and environmental conditions.

Individual and common trends are not observed directly; instead, these trends are assumed to exist and are represented as latent components in time series models. Such unobserved common components are termed "factors" (Helmut, 1993) in classical factor analysis. For the analysis of time series, dynamic factor analysis (DFA) has been applied to summarizing the information in macroeconomic analysis and to forecasting in a data-rich environment (Darné *et al.*, 2013; Ward *et al.*, 2019). The factor models are described via a spectral approach in the frequency domain (Hallin and Lippi, 2013). This approach works well when the observed time series consists of a large number of observations that can be transferred from the time domain into the frequency domain using a Fourier transformation. However, data from marine ecosystem monitoring programmes often consist of relatively short time series, for which it is thus difficult to apply frequency-based methods. As an approach to facing this challenge, Zuur *et al.* (2014) suggested the use of DFA to estimate common trends in the time domain using structural time series modelling. The approach is implemented as a general modelling framework for state space representation in the *MARSS* library of the R language (Holmes *et al.*, 2018). The state space form is a useful way to express several hidden components in the time domain, and the state is estimated by a Kalman filter or the expanded filtering theory (Shumway and Stoffer, 1982; Harvey and Pierse, 1984; Kitagawa and Gersch, 1996). Using DFA, Zuur *et al.* (2003) investigated the relationships between the estimated common trends for a biological community and environmental variables. In that work, an environmental variable was considered as an explanatory variable, and it was used for *only* the predicted biological responses that are fitted to observations. Zuur *et al.* (2003) used canonical correlations between the sea surface temperature series and common biological trends to explore possible relationships. In a canonical correlation, variations in a multivariate system are assumed to follow a stationary Gaussian process, although some formulations have proposed correcting for certain departures from the Gaussian assumption (Min and Tsay, 2005). In the case of biological and environmental variables in large marine ecosystems, it is reasonable to assume that multidecadal time series are a non-stationary process, not a stationary Gaussian process, in response to ongoing climate change and the associated biological responses.

For such non-stationary mean time series data consisting of environmental variables and biological communities, we propose a more direct approach to estimating individual trends, classifying these trends, and extracting a set of underlying common trends. We term this method *TREC*, for trend estimation and classification. The non-stationary mean time series are modelled using polynomial trend models (Solvang *et al.*, 2008) or a stochastic trend model by state space representation, commonly used as detrending models in time series analysis (Kitagawa and Gersch, 1996). Then, classification for common configurations of the trends is performed using discriminant analysis (Solvang *et al.*, 2008). The common configurations are further subdivided into sets of underlying common trends based on the target trends selected from the estimated trends. The common trends identified for each class are representative of dominant non-stationary patterns for these classes and are interpreted as common variations of biological and environmental data. TREC can be applied to

short time series data, and it is not necessary to apply a stationary Gaussian assumption to the estimated trends to investigate the relationships among them. We expect that the results can be communicated in an easily accessible form to serve the needs of multiple stakeholders. We evaluate the proposed approach using simulated datasets, including short and long time series, and apply the method to multidimensional time series observations from the ICES IEA working group for the Barents Sea (WGIBAR, ICES 2016) and the Norwegian Sea (WGINOR, ICES, 2015).

Method for *TREC*
Trend models

The observation model of a time series is given by

$$y(n) = t(n) + u(n), \quad n = 1, \cdots, N, \qquad (1)$$

where $t(n)$ is the trend component and $u(n)$ is the residual component at time step *n*. In this article, we apply two different kinds of parametric trend models: a polynomial trend model using a polynomial regression model (Solvang *et al.*, 2008) and a stochastic trend model using a *d*th order difference equation model (Kato *et al.*, 1994, 1996).

The polynomial trend model was combined with the discriminant trend analysis examined in Solvang *et al.* (2008), given by $t(n) = \beta_0 + \beta_1 n + \cdots + \beta_{p-1} n^{p-1}$ with an unknown vector $\beta \equiv (\beta_0, \beta_1, \cdots, \beta_{p-1})' \in \mathbb{R}^p$. The apostrophe symbol in vector β denotes transposition. The least squares estimator for β is given by

$$\hat{\beta}_{\mathrm{LSE}} \equiv (\mathbf{Z}\prime\mathbf{Z})^{-1}\mathbf{Z}\mathbf{Y}, \qquad (2)$$

where

$$\mathbf{Z} = \begin{pmatrix} 1, & 1, & 1^2, & \cdots, & 1^{p-1} \\ 1, & 2, & 2^2, & \cdots, & 2^{p-1} \\ & & & \vdots & \\ 1, & t, & t^2, & \cdots, & t^{p-1} \end{pmatrix} \text{and } \mathbf{Y}$$

$$\equiv \left(y(1), y(2), \cdots, y(N) \right)'. \qquad (3)$$

The trend component is estimated by

$$t(n) \equiv (1, n, n^2, \cdots, n^{p-1})\hat{\beta}_{\mathrm{LSE}}, \qquad (4)$$

which is defined on all time steps $\{1, 2, \cdots, N\}$. Assuming that the residual $u(n)$ obeys a normal distribution with variance σ^2, the estimated variance is given by

$$\begin{aligned} \hat{\sigma}^2 &= \frac{1}{N}\sum_{n=1}^{N} \left(y(n) - \hat{\beta}_0 - \hat{\beta}_1 n - \cdots - \hat{\beta}_{p-1} n^{p-1} \right)^2 \\ &= \frac{1}{N}\sum_{n=1}^{N} \left(y(n) - \hat{t}(n) \right)^2. \end{aligned} \qquad (5)$$

The log-likelihood of the polynomial trend model for this is given by

$$l(\hat{\beta}, \hat{\sigma}^2) = -\frac{N}{2}(\log 2\pi + 1 + \log \hat{\sigma}^2). \qquad (6)$$

The stochastic trend model is defined by the *d*th order difference equation, which was posed as the smoothing problem by Whittaker and Robinson (1924). This model allows for more flexible trends than does the polynomial regression model. The stochastic trend model is expressed in the following way:

$$\nabla^d t(n) = v_t(n), \qquad (7)$$

where ∇ is a difference operator $\nabla t(n) = t(n) - t(n-1)$ and $v_t(n)$ is assumed to be a white noise sequence. If $d = 1$, $t(n) \approx t(n-1)$ and the trend is known as a random walk model. If $d = 2$, $t(n) - 2t(n-1) + t(n-2) \approx 0$ (Kitagawa and Gersch, 1996). Provided that the variance of $v_t(n)$ is sufficiently small, $t(n)$ yields a smooth trend.

The model can be represented in state space form as

$$\begin{aligned} z(n) &= Fz(n-1) + Gv(n), \\ y(n) &= Hz(n) + w(n), \end{aligned} \qquad (8)$$

where $z(n)$ is the state vector corresponding to $t(n)$, $v(n)$ is the system noise vector with mean 0 and unknown variance σ_v^2, F, G, and H indicate integer or matrices, and $w(n)$ is observation error with mean 0 and unknown variance σ_w^2. The state $z(n)$ is taken as a latent factor, since we cannot directly observe it from the data. Corresponding to the above *d*th order difference equation, when $d = 1$,

$$z(n) = [t(n)], \ F = G = H = 1. \qquad (9)$$

When $d = 2$, the state vector and matrices are as follows:

$$z(n) = \begin{bmatrix} t(n) \\ t(n-1) \end{bmatrix}, \ F = \begin{pmatrix} 2 & -1 \\ 1 & 0 \end{pmatrix}, \ G = \begin{bmatrix} 1 \\ 0 \end{bmatrix}, \ \text{and } H = \begin{bmatrix} 1 \\ 0 \end{bmatrix}. \qquad (10)$$

The observation error corresponds to $u(n)$ in (1) in this case. The trend component is estimated using a Kalman filter, which is a powerful numerical algorithm that recursively operates the state estimation, prediction and filtering (Kato *et al.*, 1994, 1996):

Prediction:

$$\begin{aligned} z(n|n-1) &= Fz(n-1|n-1) \\ V(n|n-1) &= FV(n-1|n-1) + GQG', \end{aligned} \qquad (11)$$

Filtering:

$$\begin{aligned} K(n) &= V(n|n-1)H'(HV(n|n-1)H' + R)^{-1} \\ z(n|n) &= z(n|n-1) + K(y(n) - Hz(n|n-1)) \qquad (12) \\ V(n|n) &= (I - KH)V(n|n-1). \end{aligned}$$

Here, $z(n|n-1)$ and $V(n|n-1)$ are the conditional mean and conditional variance, R is the observation error, and K is Kalman gain. This trend model includes the parameter vector $\theta = (d, \sigma_v^2, \sigma_w^2)$. The log-likelihood function $l(\theta)$ of this model is given by

$$l(\theta) = \sum_{n=1}^{N} \log f(y(n)|Y(n-1), \theta),$$

$$= \sum_{n=1}^{N} \log \left. \frac{1}{\sqrt{(2\pi)^2 \det \Sigma(n)}} \exp \left(-\frac{1}{2} \Delta y(n)' \Sigma(n)^{-1} \Delta y(n) \right) \right\},$$

$$(13)$$

where $Y(n-1) = (y(1), y(2), \cdots, y(n-1))$, $\Delta y(n) = y(n) - Hz(n|n-1)$, and $\Sigma(n) = H(n)V(n|n-1)H'(n) + \sigma_w^2$. The flexibility of the estimated trend depends on σ_v^2. The optimum σ_v^2 can be determined by maximum likelihood within an arbitry variance range. The variance σ_w^2 can be directly set to the variance of the observation.

Denoting the number of parameters by c, the Akaike Information Criterion (AIC) (Akaike, 1974) value of the model, given the estimate of optimum orders p for the polynomial trend model and d for the stochastic trend model, is

$$\text{AIC}(c) = -2l(\cdot) + 2c. \tag{14}$$

The log-likelihood function can also be represented by Laplace approximation, and the optimum parameters can be estimated by a numerical optimization tool such as the AD Model Builder package (Fournier et al., 2012) or TMB (Kristensen et al., 2016).

Discrimination analysis of trends

For the estimated trend, we apply discriminant analysis, as proposed by Solvang et al. (2008). First, let us consider the following simple example of two-category discrimination:

$$\begin{aligned} \Pi_1 : & \quad \text{model (1) with trend function } T_1(n) \\ \Pi_2 : & \quad \text{model (1) with trend function } T_2(n). \end{aligned} \tag{15}$$

Suppose that we observe new data and that the trend is estimated as $\hat{t}(n)$, which is assumed to belong to Π_1 or Π_2. The classification is performed with the following divergence measure:

$$L(\hat{t} : T_j) \equiv \sum_{n=1}^{N} \{T_j(n) - \hat{t}(n)\}^2, \quad j = 1, 2. \tag{16}$$

If $L(\hat{t} : T_2) > L(\hat{t} : T_1)$, the retained category is Π_1, otherwise it is Π_2. The probability of misclassifying the observation from Π_i into Π_j $(i \neq j)$ converges to zero as $n \to \infty$. We define the discriminate function $D \equiv L(\hat{t} : T_2) - L(\hat{t} : T_1)$ for use as a discriminant score (Solvang et al., 2008). In practical use, we fix two reference trends corresponding to T_1 and T_2 and make the respective trend estimators $\hat{T}_1(n)$ and $\hat{T}_2(n)$ using model (1). For common trend classification, it is considered in practice that $\hat{T}_1(n)$ and $\hat{T}_2(n)$ represent different (opposite) shapes, namely increasing and decreasing. In other words, we assume that we can obtain a rising tendency and a declining tendency for annual changes. The different shapes result in a large distance between the two categories. Then, the discriminant function for observation $y^{(j)}(n)$, $j = 1$ to 2, is defined by

$$\hat{D}_j = \sum_{n=1}^{N} \{\hat{T}_2(n) - \hat{t}_j(n)\}^2 - \{\hat{T}_1(n) - \hat{t}_j(n)\}^2. \tag{17}$$

If $\hat{D}_j > 0$, category Π_1 is chosen, otherwise, category Π_2 is chosen. Applying the nearest neighbour method, we can classify groups according to similar $\hat{D}_j$, e.g. upward, downward, and flat,

including convex or concave. In this article, we first apply a two-category discriminant analysis to the estimated trends to roughly divide them into three groups representing configurations related to upward, flat, and downward. If it is necessary to classify them into groups of more concrete patterns from the three rough-configuration groups, this two-category classification can be easily extended to multiple-category discrimination. The problem is then specified in the following way:

$$\Pi_j : \text{model (1) with trend function } T_j(n), \quad j = 1, 2, \cdots, k. \tag{18}$$

The divergence measure in this case is given by

$$L(\hat{t} : T_j) \equiv \sum_{n=1}^{N} \{T_j(n) - \hat{t}(n)\}^2, \quad j = 1, 2, \cdots, k. \tag{19}$$

We provide a divergence measurement vector given by

$$\zeta = \left(L(\hat{t} : T_1), L(\hat{t} : T_2), \cdots, L(\hat{t} : T_k) \right). \tag{20}$$

The classification rule is defined as the requirement that the estimated trend $\hat{t}$ belong to Π_l to satisfy

$$L(\hat{t} : T_l) = \min(\zeta). \tag{21}$$

In practice, the reference trend T_j should be predefined in the three configurations groups obtained by the two-category discriminates. Finally, the reference trend T_j is assigned as a general reference, called an *icon*, which is an easily accessible form that can be used to serve the needs of stakeholders.

The entire numerical procedure and the icons we predefine in this study are summarized in Figure 1. TREC is implemented using the MATLAB code (MATLAB ver. R2018b), which is available on request.

Common trend approach by dynamic factor model

As mentioned in the Introduction, DFA is an appropriate method for analysing time series data and investigating the common trends across ecosystem components. Therefore, we refer to the approach provided by Zuur et al. (2003) and compare it with TREC. This comparison is considered in detail in the Supplementary Text.

Simulation study
Evaluation of TREC

We performed a simulation study to evaluate the performance of TREC. First, we defined two common trends $t_1(n)$ and $t_2(n)$ and a series $x_e(n)$ used as exogenous variables (Supplementary Figure S1):

$$\begin{aligned} t_1(n) &= t_1(n-1) + 0.1 \times r_{t1}(n), \\ t_2(n) &= 2 \times t_2(n-1) - t_2(n-2) + 0.5 \times r_{t2}(n), \\ x_e(n) &= 0.35 \times x_e(n-1) + 0.13 \times t_1(n) + r_e(n), \end{aligned}$$

where $r(n)$ assumes normal distribution with 0 mean and 1 standard deviation.

We then derive six variables as follows:
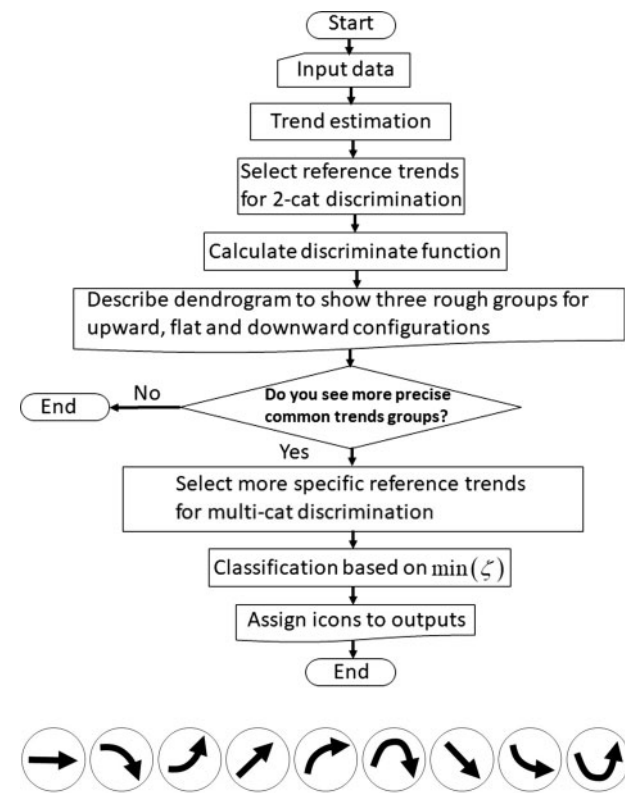
Figure 1. Flow chart of the proposed TREC procedure and predefined icons.

$$x_1(n) = 0.3 \times t_1(n) + r_1(n),$$
$$x_2(n) = t_1(n) + x_e(n) + r_2(n),$$
$$x_3(n) = -0.5 \times t_1(n) + r_3(n),$$
$$x_4(n) = 0.0004 \times t_2(n) + 0.5 \times x_e(n) + r_4(n),$$
$$x_5(n) = 0.00045 \times t_2(n) + r_5(n),$$
$$x_6(n) = 1.5 \times x_e(n) + r_6(n),$$

where $r_1(n), \cdots, r_6(n)$ are random variables normally distributed with zero mean and unit variance. We simulated series with lengths of 50- and 200-time steps (Supplementary Figure S2).

We first applied the polynomial and stochastic trend models to $x_1(n), \cdots, x_6(n)$ and $x_e(n)$. Supplementary Table S1a summarizes the calculated log-likelihood and AIC obtained by applying the stochastic trend model for $d = 1$ and $d = 2$. The results suggest that the model fits best for $d = 1$. The optimum order p (based on AIC) for the polynomial trend model and the optimum variance Q for the stochastic trend model are summarized in Supplementary Table S1b. For optimizing Q, we set $0.01 \leq Q \leq 0.1$ as a search range. This procedure was conducted for each time series, and it resulted in a set of estimated polynomial trends (Supplementary Figure S3a and b, red lines) and stochastic trends (Supplementary Figure S3c and d, red lines). The filtering of state vector $z(n)$ in the stochastic model (Supplementary Figure S3c and d, blue lines) was generally more variable than the associated polynomial trend. This is because the state vector can follow data

fluctuations according to each time point by using a Kalman filter. The prediction values usually indicated more fluctuation than the filtering values.

Next, we performed a two-category discrimination analysis. The estimated trends for x_2 and x_3 were defined as the reference trends $\hat{T}_1(n)$ and $\hat{T}_2(n)$ to calculate the discriminant function. The value obtained by the function was then used as a distance metric to perform hierarchical clustering, applying the unweighted centre of mass distance as the linkage between clusters. In Supplementary Figure S4, the dendrograms for polynomial (a and b) and stochastic trends (c and d) indicate a discrimination between upward, flat, and downward trends, which are coloured by red, blue, and black thick lines, respectively. Based on the reference trends, two categories for downward and upward were classified by $D > 0$ or $D < 0$. Some D values around 0 belonged to the flat group. In the case of data using 50 time points (Supplementary Figure S4a and c), it might be appropriate to classify the polynomial trend $x_5(n)$ into the upward configuration group rather than to the flat configuration group, while the stochastic trend of $x_5(n)$ appears slightly upward. Classifications in the case of data using 200 time points (Supplementary Figure S4b and d) indicate consistent grouping.

## Verification for discriminant function and divergence measure for $j > 2$

Solvang *et al.* (2008) mentioned the possibility that several common configuration groups were classified by the discriminant function for only the two-category setting. However, if the estimated trends present an exactly symmetrical configuration, e.g. convex and concave, both trends may be appropriate to deal with classifying in the flat condition. We demonstrated such a case using the artificial trend series generated by quadratic and exponential functions shown in Supplementary Figure S5. By selecting number 33 and 30 trends as reference trends $\hat{T}_1(n)$ and $\hat{T}_2(n)$, the two-category discriminant was considered. The bar plots for $\hat{D}_j$ are illustrated in Supplementary Figure S6. The bars in groups for upward and downward correspond to positive and negative $\hat{D}_j$ values, that is, all data can be divided into two main categories. $\hat{D}_j$ corresponding to patterns such as convex or concave is clearly indicated around 0 (Supplementary Figure S6, trends 1–20). This can be resolved using *multi*-category discrimination, with $j > 2$, as defined in previous works (18)–(20). In this case, eight-category discrimination was performed, with trends 33, 30, 1, 2, 29, 21, 38, and 32 set as the reference trends. Applying this eight-category discrimination, all data were classified into certain categories that include similar configurations as shown in Supplementary Table S2. The predefined icons set in Section 2 were also assigned according to the reference trend's patterns.

Field observations

We applied the proposed method to the time series compiled by the ICES integrated assessment working groups for the Barents Sea (WGIBAR, ICES, 2016) and the Norwegian Sea (WGINOR, ICES, 2015). Time series lengths vary among variables, so we selected the periods with continuous records (no missing data) until the final year of observation for all biotic and abiotic data. The WGIBAR dataset consists of 35 annual time series for the period 1980–2015, including 7 abiotic, 18 biotic, and 8 human impact variables. The WGINOR dataset consists of 24 annual time series

Table 1. Abbreviations used in figures and tables.

Type	Abbreviation used in figures and tables	Explanation of relevant data
a. WGIBAR data		
Abiotic	1: ArW	Area of Arctic water
	2: AW	Area of Atlantic water
	3: BSO	Barents Sea opening
	4: FB	Fugløya-Bear Island section
	5: KolaS	Salinity level in Kola section
	6: KolaT	Atlantic water temperature in Kola section
	7: NAO	Winter North Atlantic Oscillation index
Biotic	8: Jel	Jellyfish biomass, mostly *Cyanea capillata*
	9: Krill	Krill biomass
	10: Shr-a	Relative shrimp stock biomass from assessment
	11: Cap0n	Abundance 0-group capelin
	12: CapS	Capelin SSB, spawning-stock biomass
	13: CapT	Capelin TSB, stock biomass (age 1+)
	14: Her0n	Abundance 0-group herring
	15: Her1	Herring stock biomass (ages 1 and 2)
	16: Lump1	Number of lumpfish age 1 and older
	17: LumpJ	Number of juvenile lumpfish
	18: Polcd0n	Abundance 0-group polar cod
	19: Cod0n	0-group cod abundance
	20: CodRe	Recruitment of cod at age 3
	21: Cod3 + b	Cod stock biomass (age 3+)
	22: GH0n	0-group Greenland halibut abundance
	23: Had0n	0-group haddock abundance
	24: HadR3	Recruitment of herring at age 3
	25: HadSSB	Spawning-stock biomass of haddock, ages 6–8
Human impact	26: CdF510	Fishing mortality of cod, ages 5–10
	27: HadF47	Fishing mortality of haddock, ages 4–7
	28: RelFc	Relative fishing mortality calculated as sum of catches of capelin in fall and next spring divided by biomass in August/September
	29: RelFS	Relative fishing mortality of shrimp
	30: HarpSL	Landings of harp seals
	31: MinL	Landings of minke whales
	32: PolcdL	Landings of Barents Sea polar cod
	33: ShrL	Landings of shrimp in Barents Sea
b. WGINOR data		
Abiotic	1: NAO	Winter North Atlantic Oscillation index
	2: SPGw	Sub-polar gyre index from satellite ssh data, centred in January
	3: NLgy	Area averaged wind stress curl within 2 000-m isobaths in Norwegian Sea
	4: SvicT	Temperature in layer 50–200 m, using stations over 1 010-, 1 075-, and 1 185-m depths in Svinoy section
Biotic	5: MaxN	Maximum chlorophyll a level in Norwegian basin
	6: MaxL	Maximum chlorophyll a level in Lofoten basin
	7: HerR	Recruitment of herring per year class at age 2
	8: BWR	Recruitment of blue whiting per year class at age 1
	9: MacR	Recruitment of mackerel per year class at age 0
	10: HerB	Spawning-stock biomass of herring
	11: BWB	Spawning-stock biomass of blue whiting
	12: MacB	Spawning-stock biomass of mackerel
	13: BRedB	Spawning-stock biomass of beaked redfish
	14: SaiB	Large saithe (9+ for North Sea and Faroese stocks and 10+ for Northeast Arctic stock)
	15: HerrW6	Weight at age 6 in herring stock
	16: BWW6	Weight at age 6 in blue whiting catch
	17: MacW6	Weight at age 6 in mackerel stock
	18: Puff	Puffin stock size by sum of counts from Runde, Sklinna, Røst, and Anda
	19: Kitw	Kittywake stock size by sum of counts from Runde, Sklinna, Røst, and Anda
	20: Guill	Guillemoth stock size by sum of counts from Runde and Røst
	21: ZB48W	Zooplankton biomass in Norwegian Sea
	22: ZBB	Zooplankton biomass in Lofoten and Norwegian basins
	23: ZNEI	Zooplankton, northeast of Iceland
	24: GHB	Greenland halibut biomass and >45 cm body length
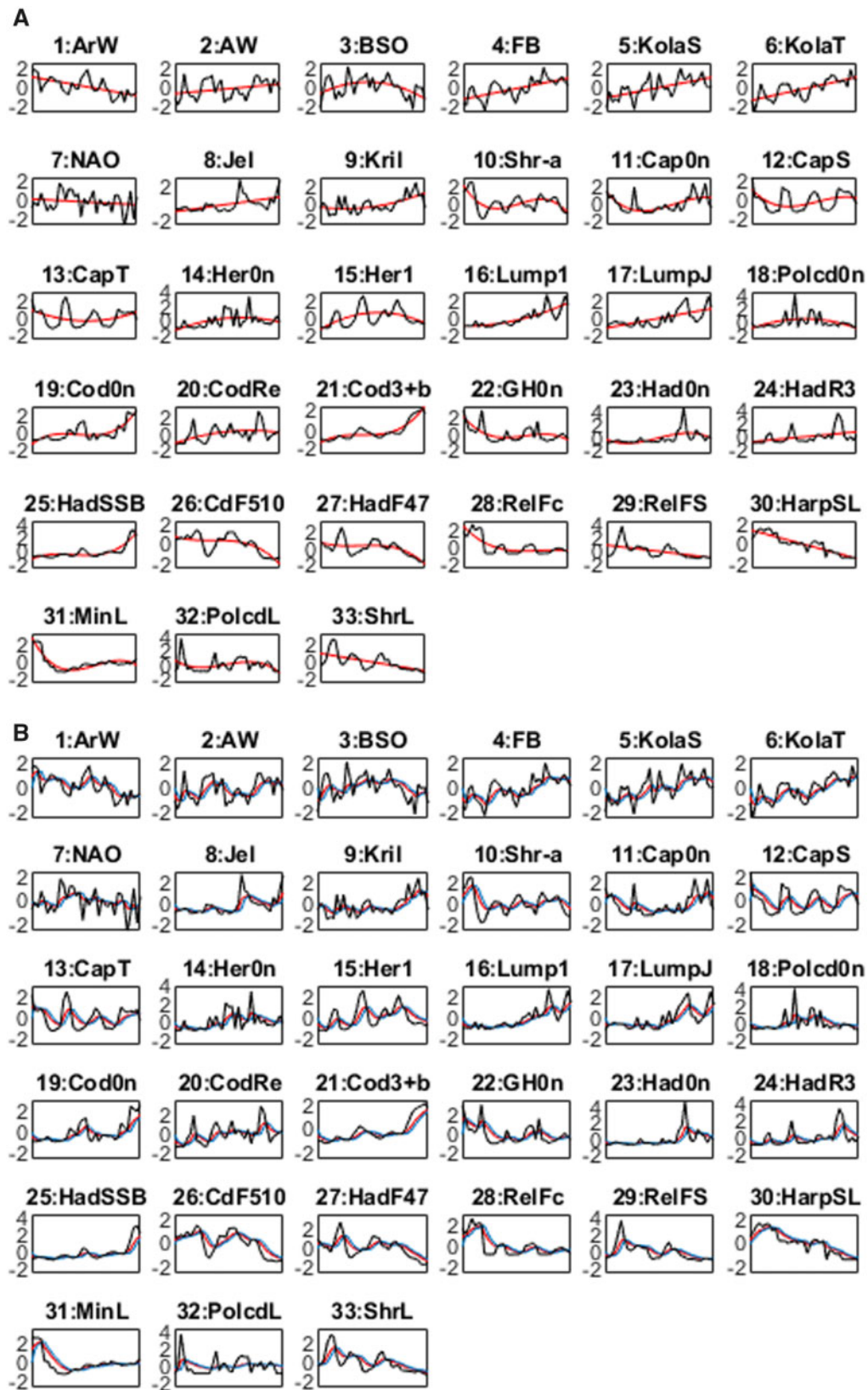
Figure 2. Estimated trends in applying polynomial and stochastic trend models to WGIBAR dataset, which consists of 35 annual time series for the period 1980–2015. (a) Estimated polynomial trends (red: trend, black: observation). (b) Estimated stochastic trends (red: prediction, blue: filtering, black: observation).
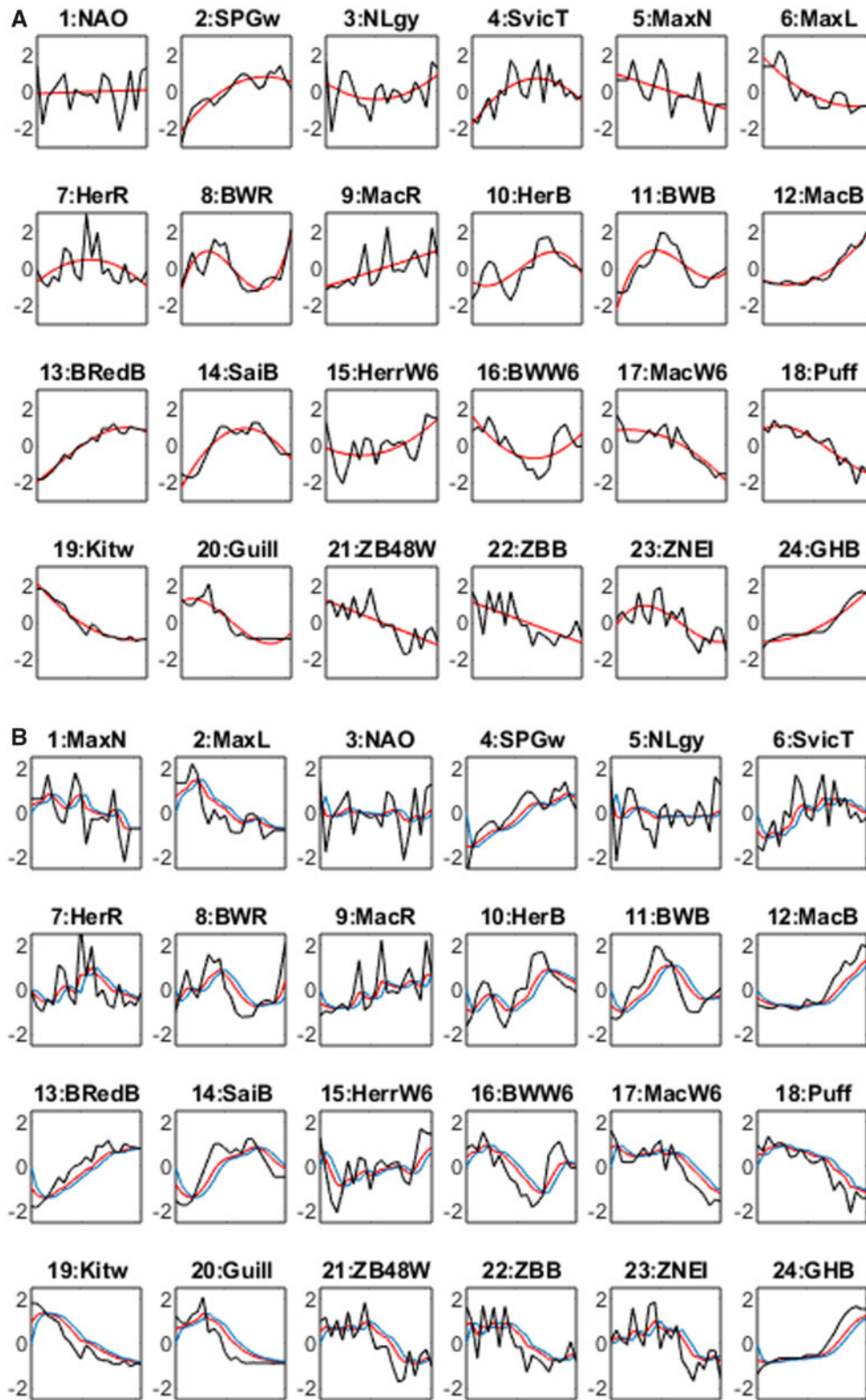
Figure 3. Estimated trends in applying polynomial and stochastic trend models to WGINOR dataset, which consists of 24 annual time series for the period 1995–2015. (a) Estimated polynomial trends (red: trend, black: observation). (b) Estimated stochastic trends (red: prediction, blue: filtering, black: observation).

Table 2. Results of discrimination analysis for WGIBAR data: three common configuration groups of trends by two-category discriminates and the assigned data.

Common trend configuration	Abiotic	Biotic	Human impact
Upward	2: AW, 4: FB, 5: KolaT, 6: KolaS	8: Jel, 9: Kril, 11: Cap0n, 14: Her0n, 16: Lump1, 17: LumpJ, 19: Cod0n, 20: CodRe, 21: Cod3 + b, 23: Had0n, 24: HadR3, 25: HadSS	–
Flat	3: BSO, 7: NAO	10: Shr-a, 12: Cap S, 13: CapT, 15: Her1, 18: Polcd0n	31: MinL, 32: PolcdL
Downward	1: ArW	22: GH0n	26: CdF51, 27: HadF47, 28: RelFc, 29: RelFS, 30: HarpSL

Table 3. Results of discrimination analysis for WGINOR data: three common configuration groups of trends by two-category discriminates and the assigned data.

Common trend configuration	Abiotic	Biotic
Upward	4: SPGw, 6: SVicT	9: MacR, 10: HerB, 12: MacB, 13: BRedB, 14: SaiB, 15: HerrW6, 24: GHB
Flat	3: NAO, 5: NLgy	7: HerR, 8: BWR, 11: BWB, 16: BWW6
Downward		1: MaxN, 2: MaxL, 17: MacW6, 18: Puff, 19: Kitw, 20: Guill, 21: ZB48W, 22: ZBB, 23: ZNEI

for the period 1995–2015, including 6 abiotic and 18 biotic variables. The abbreviations of individual time series variables are listed in Table 1, including the data that are missing less than three time points.

Results and discussion

The stochastic trend models with $d = 1$ outperformed the stochastic trend model for $d = 2$, for both datasets, as indicated by the AIC values (Supplementary Figure S7a for WGIBAR and Supplementary Figure S7b for WGINOR). The estimated polynomial and stochastic trends visible in Figure 2 (WGIBAR) and Figure 3 (WGINOR) and the optimum numbers of parameters are summarized in Supplementary Table S4. While the order of polynomial trend models can vary among individual time series, the values of optimum Q are mainly equal to 0.1, reflecting the fact that flexible stochastic trends are predominantly selected.

The clustering of trends is visualized in Supplementary Figures S8 (WGIBAR) and S9 (WGINOR). The classification procedure via discriminant analysis requires the pre-selection of reference trends. As mentioned, the reference trends for the two-category discriminant should be clearly opposite shapes, such as upward and downward. For WGIBAR, trends 16 (number of lumpfish age 1+) and 30 (landings of harp seals) were used as references for both polynomial and stochastic trend models. For WGINOR, trends 5 (Maximum chlorophyll a level in Norwegian basin) and 9 (recruitment of mackerel) were used as references for polynomial trend models, and trends 2 (sub-polar gyre index from satellite ssh data) and 18 (puffin stock size) were used as references for stochastic trend models.

The trends were first divided into two categories and further classified into three categories: upward, flat, and downward. Tables 2 and 3 list the abiotic and biotic data for the common configurations. For most individual trends, the classification into upward, flat, and downward groups was consistent between the polynomial and the stochastic trend models. A few trends were exceptions to this general pattern: while in the WGIBAR analysis polynomial trend 15 (ages 1 and 2 herring stock biomass) was

convex and polynomial trend 31 (Landings of minke whales) was concave, the corresponding stochastic trends 15 and 31 display more fluctuations and are not discriminated into flat configurations. Similar tendencies were observed in trends 8 (recruitment of blue whiting per year class at age 1), 15 (weight at age 6 in herring stock), and 16 (weight at age 6 in blue whiting catch) for WGINOR. The simulation study in the case of 50 time points also indicated inconsistent classification in Supplementary Figure S4a and b. This suggests that a polynomial trend could be handled in a simpler way to assign trend estimates to several icon configurations using multi-category discrimination.

Using polynomial trend estimates, we set more reference trends in the three groups and classified all trends precisely into groups by multi-category discrimination. The subdivided outputs in three common trends are summarized in Figure 4 for WGIBAR and Figure 5 for WGINOR. Tables 4 and 5 list the details for classified data in each category. To each classified trend, we associated an icon representation that could be used to simply and efficiently communicate information on long-term changes in variables. The estimated trends by the polynomial model present rough long-term changes and may be more useful for assigning icons. On the other hand, the estimated trend by the stochastic trend model can follow more precise changes according to data fluctuations. Therefore, analysers could select the polynomial or stochastic trend model to investigate long-term changes in their data depending on their aim or interest.

The icons presented in Table 4 highlight the observation that in the Barents Sea there has been a continuous increase in temperature. It is visible in the increasing temperature trends in the Bear Island trough (4) and the Kola section (6) and in the increasing extent of the area occupied by Atlantic water (2) as well as the decreasing trend in the extent of area occupied by Arctic water (1). These changes have been paralleled by increases in the biomass of jellyfishes (8), the abundance of juvenile lumpsuckers (17), and haddock recruitment (24) and by decreases in fishing mortality of shrimps (29) and landings of shrimps (33) and harp seals (30). The increasing trends in krill biomass (9) and
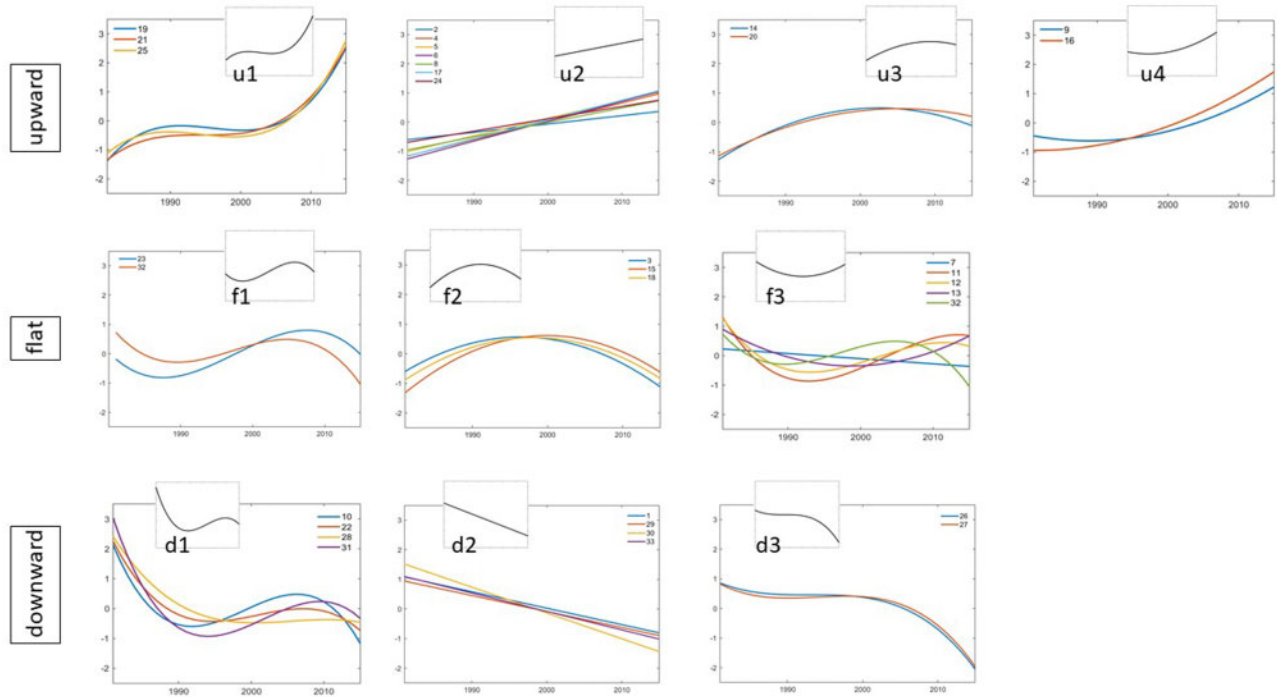
Figure 4. Subdivided common trends in three groups for WGIBAR data. The reference trends are assigned to the icons in Table 4 as follows: u1: 25.HadSSB, u2: 24.HadR3, u3: 20.CodRe, u4: 9.Krill, f1: 23.Had0n, f2: 15.Her1, f3: 13.CapT, d1:31.ShrL, d2:30.HarpSL, and d3:26.CdF510.
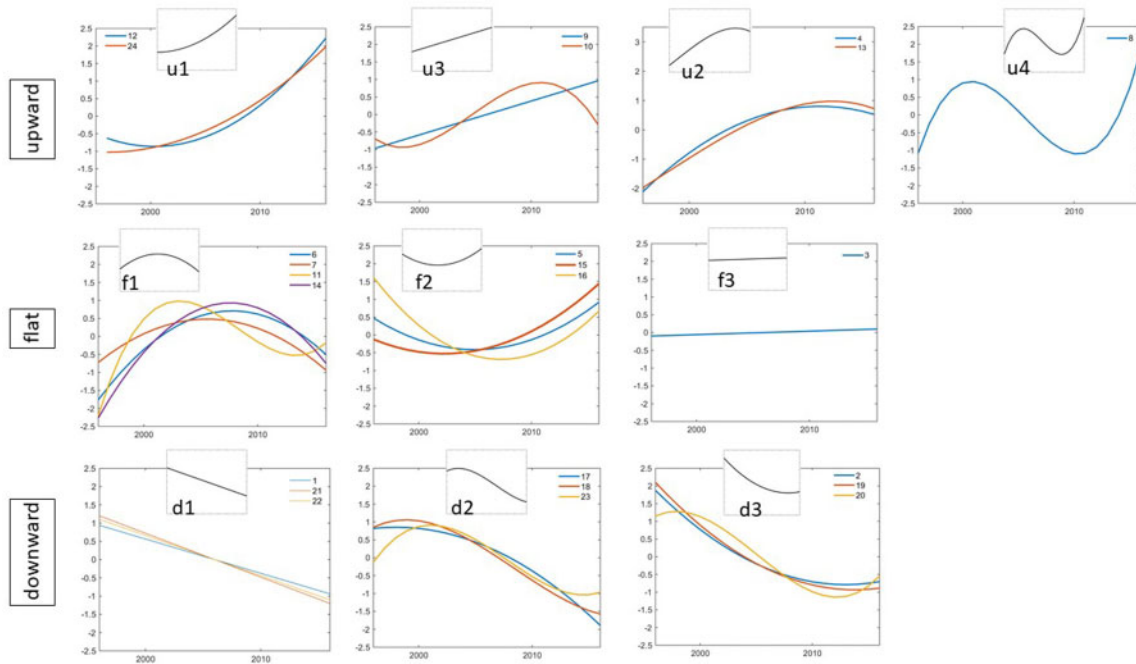
Figure 5. Subdivided common trends in three groups for WGINOR data. The reference trends are assigned to the icons in Table 5 as follows: u1: 24.GHB, u2: 9.MacR, u3: 13.BRedB, u4: 8.BWR, f1: 7.HerR, f2: 5.MaxN., f3: 3.NLgy, d1:22.ZBB, d2:18.Puff, and d3:2.SPGw.

abundance of age 1+ lumpsuckers (16) have been accelerating, while the increasing trends in cod (20) and herring (14) recruitment have been decelerating. Furthermore, the decreasing trend in fishing mortality of adult cod (26) and haddock (27) has been accelerating in recent years. A similar understanding of trends in

the main abiotic, biotic, and human factors in the Norwegian Sea can be achieved based on the icons presented in Table 5. As seen by these interpretations of the outputs, these icons can be used in ecological "dashboards" displaying a list providing summaries of ecological states and trends.

Table 4. Results of discrimination analysis for WGIBAR data: assigned icons by multi-category discriminates.

Common trend configuration	Category	Classified data	Icon
Upward		19:Cod0n, 21:Cod3+b, 25:HadSSB	
		2:AW, 4:FB, 5:KolaS, 6:KolaT, 8:Jel, 17:LumpJ, 24:HadR3	
		14:HerOn, 20:CodRe	
		9:Kril, 16:Lump1	
Flat		23:Had0n, 32:PolcdL	
		3:BSO, 15:Her1, 18:Polcd0n	
		7:NAO, 11:Cap0n, 12:CapS, 13:CapT, 32:PolcdL	
Downward		10: Shr-a, 22:GH0n, 28:RelFc, 31:MinL	
		1:ArW, 29:RelFS, 30:HarpSL, 33:ShrL	
		26:CdF51, 27:HadF47	

Table 5. Results of discrimination analysis for WGINOR data: assigned icons by multi-category discriminates.

Common trend configuration	category	Classified data	Icon
Upward		12:MacB, 24:GHB	
		2:SPGw, 13:BRedB	
		9:MacR, 10:HerB	
		8:BWR	?
Flat		4:SvicT, 7:HerR, 11:BWB, 14:SaiB	
		3:Nlgy, 15:HerrW6, 16:BWW6	
		1:NAO	
Downward		5:MaxN, 21:ZB48W, 22:ZBB	
		17:MacW6, 18:Puff, 23:ZNEI	
		6: MaxL, 19:Kitw, 20:Guill	

The combination of trend identification, classification, and icon representations provides an easily accessible representation of the trends in abiotic, biotic, and human factors, which can support discursive interpretations while still being rooted in an objective statistical approach.

In reality, the majority of marine ecosystems do not have complete datasets for a full time series to be analysed. For such missing data, the provided trend models support he interpolation of them. In the case of a polynomial trend model, Solvang *et al.* (2008) showed the interpolated trend estimates and the classification. Furthermore, the stochastic trend model can fill the missing data in the Kalman filter recursions (Kitagawa and Gersch, 1996).

Considering the meaning of *common trend*, the dominant trend's configuration presents long-run movements towards comprehensive data and it may be useful for a biologist or ecologist if the fluctuations in environmental factors and fish communities could be easily interpreted as upward, flat, or downward. In the case of analysis by the DF model (Zuur *et al.*, 2014) summarized in Supplementary Text, the obtained common factors include several patterns mixing long-term trend and cyclic fluctuations, and thus, it may be difficult to interpret the physical meaning of such factors. Since most relevant observations have a small sample size of data points in the time series data, comparing configurations may provide a simple and useful way to gain a preliminary understanding of an ecosystem. TREC helps to provide a simple interpretation of which trend pattern is dominant over all relevant data for abiotic and biotic cases. When we predefined the reference trends used for discrimination, no prior knowledge was considered, that is, it was simply done in an arbitrary manner in this article. However, it would also be possible to predefine reference trends based on the prior knowledge of marine biologists or ecologists.

Conclusion

TREC is proposed as an approach to analysing common trends in a marine ecosystem. It consists of two procedures: (i) estimating trends with statistical trend models and (ii) classifying the estimated trends into categories of common configurations. The classification step enables us to find specific configurations by representing the estimated trend patterns. A simulation clarified the performances of two different trend models and their flexibility for use with several representative patterns, which can be predefined as icons. We applied TREC to two real time series datasets provided by the ICES integrated assessment working groups. Abiotic, biotic, and human impact data were classified into common trend groups. The proposed TREC focuses on long-term trends of data, and it works for any length of time steps. TREC could become a methodology established for ITA in IEA by validation through benchmarking practices. Studies conducted to investigate precise ecosystem functions using TREC are expected as further extensions of this work.

Supplementary data

Supplementary material is available at the *ICESJMS* online version of the manuscript.

References

Akaike, H. 1974. A new look at the statistical model identification. IEEE Transactions on Automatic Control, 19: 716–723.

Darné, O., Barhoumi, K., and Ferrara, L. 2013. Dynamic factor models: a review of the literature. OECD Journal: Journal of Business Cycle Measurement and Analysis, 2013: 73–107.

DePiper, G. S., Gaichas, S. K., Lucey, S. M., Pinto da Silva, P., Anderson, M. R., Breeze, H., Bundy, A. *et al.* 2017. Operationalizing integrated ecosystem assessments within a multidisciplinary team: lessons learned from a worked example. ICES Journal of Marine Science, 74: 2076–2086.

Fournier, D. A., Skaug, H. J., Ancheta, J., Ianelli, J., Magnusson, A., Maunder, M. N., Nielsen, A. *et al.* 2012. AD model builder: using

automatic differentiation for statistical inference of highly parameterized complex nonlinear models. Optimization Methods and Software, 27: 233–249.

Hallin, M., Hörmann, S., and Lippi, M. 2018. Optimal dimension reduction for high-dimensional and functional time series. Statistical Inference for Stochastic Processes, 21: 385–398.

Hallin, M., and Lippi, M. 2013. Factor models in high-dimensional time series—a time-domain approach. Stochastic Processes and Their Applications, 123: 2678–2695.

Hardison, S., Perretti, C. T., DePiper, G. S., and Beet, A. 2019. A simulation study of trend detection methods for integrated ecosystem assessment. ICES Journal of Marine Science, 76: 2060–2069.

Harvey, A. C. 1989. Forecasting, Structural Time Series Models and Kalman Filter. Cambridge University Press, Cambridge.

Harvey, A. C., and Pierse, R. G. 1984. Estimating missing observations in economic time series. Journal of the American Statistical Association, 79: 125–131.

Helmut, L. 1993. Introduction to Multiple Time Series Analysis, 2nd edn. Springer-Verlag, New York.

Hilborn, R., and Walters, C. J. 1992. Quantitative Fisheries Stock Assessment. Choice, Dynamics and Uncertainty. Chapman and Hall, Inc., New York. 570 pp.

Holmes, E. E., Ward, E. J., and Scheuerell, M. D. 2018. Analysis of Multivariate Time Series Using the MARSS Package. Northwest Fisheries Science Center, NOAA, Seattle, WA.

ICES. 2013. World Conference on Stock Assessment Models (WCSAM). ICES Document CM 2013/ACOM/SCICOM: 02.

ICES. 2015. Final Report of the Working Group on the Integrated Assessment of the Norwegian Sea (WGINOR). ICES Document CM 2015/SSGIEA: 10. 149 pp.

ICES. 2016. Final Report of the Working Group on the Integrated Assessment of the Barents Sea (WGIBAR). ICES Document CM 2016/SSGIEA: 04. 123 pp.

ICES. 2018. Report of the Workshop on Integrated Trend Analyses in Support to Integrated Ecosystem Assessment (WKINTRA). ICES Document CM 2018/IEASG: 15. 23 pp.

Kato, H., Naniwa, S., and Ishiguro, M. A. 1996. Bayesian multivariate nonstationary time series model for estimating mutual relationships among variables. Journal of Econometrics, 75: 147–161.

Kato, H., Wada, T., and Ishiguro, M. 1994. A study of human body balance by new multivariate feedback models with common low frequency components. Japanese Journal of Biometrics, 15: 41–57.

Kawasaki, Y. 2004. Smoothness priors analysis of economic and financial time series, section 6, 215866. Doctoral dissertation, Tokyo University.

Kitagawa, G., and Gersch, W. 1996. Smoothness Priors Analysis of Time Series. Lecture Notes in Statistics 116. Springer-Verlag, New York.

Kristensen, K., Nielsen, A., Berg, C. W., Skaug, H. J., and Bell, B. M. 2016. TMB: automatic differentiation and Laplace approximation. Journal of Statistical Software, 70: 1–21.

Levin, P. S., Fogarty, M. J., Murawski, S. A., and Fluharty, D. 2009. Integrated ecosystem assessments: developing the scientific basis for ecosystem-based management of the ocean. PLoS Biology, 7: e14.

Levin, P. S., Kelble, C. R., Shuford, R. L., Ainsworth, C., deReynier, Y., Dunsmore, R., Fogarty, M. J. *et al. 2014.* Guidance for implementation of integrated ecosystem assessments: a US perspective. ICES Journal of Marine Science, 71: 1198–1204.

MATLAB ver R. 2018b. The MathWorks Inc., Natick, MA.

Min, W., and Tsay, R. S. 2005. On canonical analysis of multivariate time series. Satistica Sinica, 15: 303–323.

Planque, B., and Arneberg, P. 2018. Principal component analyses for integrated ecosystem assessments may primarily reflect methodological artefacts. ICES Journal of Marine Science, 75: 1021–1028.

Shumway, R. H., and Stoffer, D. S. 1982. An approach to time series smoothing and forecasting using the EM algorithm. Journal of Time Series Analysis, 3: 253–264.

Solvang, H. K., Subbey, S., and Frank, A. S. J. 2017. Causal drivers of Barents Sea capelin (*Mallotus villosus*) population dynamics on different time scales. ICES Journal of Marine Science, 75: 621–630.

Solvang, H. K., and Subby, S. 2018. Causal inference for marine ecosystem based on the total power Contribution. Proceedings of the Institute of Statistical Mathematics, 66: 319–337.

Solvang, H. K., and Subbey, S. 2019. An improved methodology for quantifying causality in complex ecological systems. PLoS One, 14: e0208078.

Solvang, H. K., Taniguchi, M., Nakatani, T., and Amano, S. 2008. Classification and similarity analysis of fundamental frequency patterns in infant spoken language acquisition. Statistical Methodology, 5: 187–208.

Vanhatalo, E., and Kulahci, M. 2016. Impact of autocorrelation on principal components and their use in statistical process control. Quality and Reliability Engineering International, 32: 1483–1500.

Ward, E. J., Anderson, S. C., Daminano, L. A., Hunsicker, M. E., and Litzow, M. A. 2019. Modeling regimes with extremes: the bayesdfa package for identifying and forecasting common trends and anomalies in multivariate time-series data. The R Journal, 11: 46–55.

West, M., and Harrison, J. 1997. Bayesian Forecasting and Dynamic Models, Springer Series in Statistics. Springer-Verlag, New York.

Whittaker, E. T., and Robinson, G. 1924. The Calculus of Observations, a Treasure on Numerical Calculations. Blackie and Son, Limited, London.

Zuur, A. F., Fryer, R. J., Jolliffe, I. T., Dekker, R., and Beukema, J. J. 2003. Estimating common trends in multivariate time series using dynamic factor analysis. Environmetrics, 14: 665–685.

Zuur, A. F., Tuck, I. D., and Bailey, N. 2014. Dynamic factor analysis to estimate common trends in fisheries time series. Canadian Journal of Fisheries and Aquatic Science, 60: 542–552.

Handling editor: Jason Link